chemosensors

MDPI

Article

A Metal Organic Framework-Based Light Scattering ELISA for the Detection of Staphylococcal Enterotoxin B

Kai Mao [1,†], Lili Tian [1,†], Yujie Luo [1], Qian Li [2], Xi Chen [1], Lei Zhan [2], Yuanfang Li [1], Chengzhi Huang [2] and Shujun Zhen [1,*]

[1] Key Laboratory of Luminescence Analysis and Molecular Sensing (Southwest University), Ministry of Education, College of Chemistry and Chemical Engineering, Southwest University, Chongqing 400715, China; mk1534@email.swu.edu.cn (K.M.); tianlili123@email.swu.edu.cn (L.T.); lyj0712@email.swu.edu.cn (Y.L.); cx961019@email.swu.edu.cn (X.C.); liyf@swu.edu.cn (Y.L.)

[2] Key Laboratory of Luminescent and Real-Time Analytical Chemistry (Southwest University), Chongqing Science and Technology Bureau, College of Pharmaceutical Sciences, Southwest University, Chongqing 400715, China; lq671225@email.swu.edu.cn (Q.L.); zhanlei6@swu.edu.cn (L.Z.); chengzhi@swu.edu.cn (C.H.)

* Correspondence: zsj@swu.edu.cn

† These authors contributed equally to this work.

Abstract: Enzyme-linked immunosorbent assay (ELISA) is one of the most commonly used method for the detection of staphylococcal enterotoxin B (SEB), the main protein toxin causing staphylococcal food poisoning. However, the traditional ELISA reaction needs to be stopped by sulfuric acid to obtain stable colorimetric signal, and it is easily influenced by a colored sample. In order to address this problem, a new ELISA method using zeolite imidazolate skeleton-8 metal-organic framework (ZIF-8 MOF) as a light scattering (LS) reporter for SEB detection was developed in this work. ZIF-8 MOF has the characteristics of high porosity, large specific surface area, clear pore structure, and adjustable size, which is one of the most representative MOFs constructed from Zn^{2+} and 2-methylimidazole (2-mIM). The 2-mIM ligand of ZIF-8 exhibited antioxidant activity and can strongly react with H_2O_2, which could destroy the structure of ZIF-8, resulting in the obvious decrease in LS intensity. We combined this specific reaction with the sandwich immune reaction to construct the LS ELISA method for the successful detection of SEB. This method is more reliable than commercial tests kits for the detection of colored samples, and it is simple, sensitive, and selective, and has great potential in the detection of other toxins by simply changing the corresponding recognition units.

Keywords: ELISA; light scattering; metal organic framework; ZIF-8; staphylococcal enterotoxin B

Citation: Mao, K.; Tian, L.; Luo, Y.; Li, Q.; Chen, X.; Zhan, L.; Li, Y.; Huang, C.; Zhen, S. A Metal Organic Framework-Based Light Scattering ELISA for the Detection of Staphylococcal Enterotoxin B. *Chemosensors* **2023**, *11*, 453. https://doi.org/10.3390/chemosensors11080453

Academic Editor: Francesco Baldini

Received: 25 June 2023
Revised: 8 August 2023
Accepted: 10 August 2023
Published: 13 August 2023

1. Introduction

Staphylococcal enterotoxin B (SEB) is one of the main protein toxins causing staphylococcal food poisoning [1]. It is resistant to high temperature, acid, and alkali, and easy to formulate as an aerosol. It has been not only linked to food poisoning but also classified as a potential Class B biological warfare agent by the US Centers for Disease Control and Prevention (CDC). Therefore, it is highly important to develop sensitive method to detect SEB. The traditional SEB detection methods include chromatography [2], mass spectrometry [3,4], spectral method [5], electrochemical method [6], Raman spectroscopy [7], enzyme-linked immunosorbent assay (ELISA) [8], and so on. At present, the detection limit of SEB reported in the literature has been as low as 4.29 fg/mL [9]. Among these methods, ELISA has attracted a lot of attention because of its high sensitivity, throughput, and specificity. Generally, the ELISA method for SEB detection depends on the double-antibody sandwich system and the colorimetric signal is produced by the specific reaction between 3,3′,5,5′-Tetramethylbenzidine (TMB) and H_2O_2 catalyzed by horseradish peroxidase (HRP) that is labelled to the secondary antibody. Although this reaction is highly efficient, it

needs to be stopped by sulfuric acid, which is highly corrosive. In addition, the signal of colorimetric ELISA is easily influenced by a colored sample. Therefore, it is necessary to develop a new ELISA method for the detection of SEB.

Light scattering (LS) signal [10–12], which can be easily detected using a spectrofluorometer, has been widely used for biosensing [13–18] and chemosensing [19,20]. According to the Rayleigh scattering principle [21,22], the LS intensity of a nanoparticle strongly depends on its size [23,24]. The larger the particle size, the stronger the LS intensity. Thus, the significant differences in LS between the larger and smaller nanoparticles could be applied for analytical purposes. Furthermore, the colored molecules in samples does not influence the LS intensity of nanoparticles with large sizes [25]. However, to the best of our knowledge, there is no report on the coupling of the LS technique with ELISA for the detection of biotoxins.

As a kind of special porous material, metal-organic frameworks (MOFs) have the characteristics of high porosity, large specific surface area, clear pore structure, and adjustable size [26,27]. Zeolite imidazolate skeleton-8 (ZIF-8) is one of the most representative MOFs, which is constructed from Zn^{2+} and 2-methylimidazole (2-mIM) [28,29]. According to the previous reports, the 2-mIM ligand of ZIF-8 exhibited antioxidant activity and can react with H_2O_2 strongly, which will destroy the structure of ZIF-8 [30,31]. ZIF-8 itself has a high LS intensity because of its large size [32,33]. After the reaction with H_2O_2, the LS signal of ZIF-8 will decrease significantly. Thus, ZIF-8 is expected to be used as a novel LS reporter for analysis and detection. Furthermore, ZIF-8 has several outstanding characteristics. Firstly, the synthesis of ZIF-8 is simple and cost-effective. Secondly, the size of ZIF-8 is tunable by adjusting its synthesis conditions. Thirdly, ZIF-8 has large surface area and numerous reaction sites.

Inspired by above reports, we developed a new ELISA method for SEB detection using ZIF-8 as a LS reporter in this work. Quantitative detection of SEB can be achieved by the significantly changed LS intensity of ZIF-8. This method does not need a strong acid to stop the reaction and is not influenced by a colored sample, and it has been successfully applied for the SEB detection in complex sample, showing great potential in food safety testing.

2. Materials and Methods

2.1. Chemicals and Apparatus

The 2-methylimidazole (2-mIM) was obtained from Shanghai Aladdin Biochemical Technology Co., Ltd. (Shanghai, China). The zinc nitrate hexahydrate ($Zn(NO_3)_2 \cdot 6H_2O$) was purchased from Chengdu Chron Chemicals Co., Ltd. (Chengdu, China). Hydrogen peroxide (H_2O_2) and ethanol were purchased from Chuandong Chemical Group Co. Ltd. (Chongqing, China). The staphylococcal enterotoxin B (SEB) and staphylococcal enterotoxin A (SEA) were obtained from Pumai Biotechnology Co., Ltd. (Shanghai, China). The SEB test kits were obtained from Nanjing Herb Source Biotechnology Co., Ltd. (Nanjing, China). Glycine, ochratoxin A (OTA), Aflatoxin B1 (AFB1), carcinoembryonic antigen (CEA), and hemoglobin (HGB) were purchased from Subosen Biotechnology Co., Ltd. (Chengdu, China), and the bovine serum albumin (BSA) was purchased from Sigma Aldrich Trading Co., Ltd. (Shanghai, China). The orange juice (Nongfu spring), skim milk powder (anchor), and fresh milk (Tianyou) were purchased from the YongHui supermarket (Chongqing, China). The sample dilution buffer (0.1 mol/L PBS, pH 7.4, 0.1% Tx-100) was prepared in the laboratory. Millipore Milli-Q water (18.2 MΩ) was used in all experiments. All the other chemicals were of analytical grade and used without further purification.

The light scattering signals were measured with an F-2500 fluorescence spectrophotometer (Hitachi, Japan) by simultaneously scanning the excitation and emission monochromator of the spectrofluorometer with same starting excitation and emission wavelength (namely, $\lambda_{em} = \lambda_{ex}$). Vacuum drying oven (DZF-6020, Keelrein, Shanghai, China) was used to dry ZIF-8. The scanning electron microscope (S-4800, Hitachi, Tokyo, Japan) was utilized to measure the morphology of ZIF-8. Dark field microscopy imaging was obtained using a BX51 light microscope (Olympus, Tokyo, Japan) equipped with a dark field con-

denser (U-DCW, Olympus, Japan). The Fourier transform infrared spectrometer Prestige-21 (FTIR, Shimadzu, Kyoto, Japan) was used to test the infrared spectra of materials. X-ray diffractometer D8 ADVANCE (Brock, Germany) was used to test powder X-ray diffraction patterns of samples in a scanning range of 5–50 θ at a scanning speed of 1.5 °/min.

2.2. Synthesis of ZIF-8

The synthesis method of ZIF-8 was according to the reported literature with little modification [34]. First, 1.32 mol/L 2-mIM and 24 mmol/L $Zn(NO_3)_2{\cdot}6H_2O$ were prepared using water as solvent using ultrasonic dissolution for 10 min. Next, 500 µL of 1.32 mol/L 2-mIM was added to the glass sample bottle and pre-stirred for 30 s, and then, 500 µL of 24 mmol/L $Zn(NO_3)_2{\cdot}6H_2O$ was added. After being stirred for 5 min, the mixture was kept stagnant for 1 h. After washing twice with ethanol, the as-prepared ZIF-8 was stored at 4 °C for further use.

2.3. Dark Field Light Scattering Imaging of the Reaction between ZIF-8 and H_2O_2

The reaction process of ZIF-8 and H_2O_2 was monitored using a dark field light scattering microscope. The cationic slides were rinsed with ultrapure water and dried with nitrogen. Then, 100 µL of 50 µg/mL ZIF-8 ethanol solution was added to the surface of the cationic glass slide and was allowed to stand at room temperature for 15 min to facilitate ZIF-8 deposition on the surface of the cationic glass slide. The excess solution on the surface of the slides was then rinsed with ultrapure water and blow-dried with nitrogen. In order to monitor the reaction between ZIF-8 and H_2O_2 in real-time, 200 µL ethanol solution was added between the slides and cover slides to obtain the original dark field image of ZIF-8. Next, ethanol solution was removed and 200 µL of 3% H_2O_2 solution was added. Then, dark field microscopic images of the reaction process between ZIF-8 and H_2O_2 were collected.

2.4. Detection of SEB

The light scattering ELISA method was developed based on the ELISA tests kits. A 50 µL volume of different concentrations of SEB were added to the 96-well plate pre-modified with Ab1 of SEB. Then, 100 µL of HPR-Ab2 was added and incubated at 37 °C for 1 h. Each well of the 96-well plate was washed with 350 µL washing buffer five times to remove the uncombined SEB and HRP-Ab. The above steps were consistent with the operation of the ELISA test kits. Then, 100 µL of 6% H_2O_2 was added to each well and incubated for 15 min in a 37 °C incubator. The residual 100 µL H_2O_2 of the reaction was transferred to the pre-ultrasonicated, dispersed 100 µL of 100 µg/mL ZIF-8 solution and reacted at room temperature. Finally, the LS spectrum was obtained using F-2500.

3. Results and Discussion

3.1. Principle of the SEB Detection

The SEB detection principle is shown in Figure 1. Firstly, ZIF-8 was synthesized using 2-mIM as the ligand and Zn^{2+} as the central ion. As the ligand 2-mIM could be oxidized by H_2O_2, the structure of ZIF-8 could be destroyed by H_2O_2, and the LS intensity was reduced. Subsequently, we combined this reaction with SEB antibody immune sandwich assay to construct a new SEB detection method. When SEB was added, an Ab1/SEB/Ab2-HRP sandwich immune structure formed in the 96-well plate. After the addition of H_2O_2 into the 96-well plate, the H_2O_2 was consumed by the HRP on Ab2. Then, the residual H_2O_2 after the reaction was transferred to the ZIF-8 solution. Since H_2O_2 was consumed by HRP, the oxidation ability of H_2O_2 toward 2-mIM was weak. And ZIF-8 maintained an intact structure, showing high LS intensity. When there was no SEB in the system, the sandwich immune structure cannot be formed, and the added H_2O_2 will not be consumed by HRP. In this situation, the amount of H_2O_2 was large, and the oxidation capacity of H_2O_2 toward 2-mIM was strong, leading to the damage of the structure of ZIF-8 and resulting

in the decreased LS intensity. Thus, quantitative detection of SEB can be achieved by the obviously changed LS intensity of ZIF-8 before and after adding SEB.

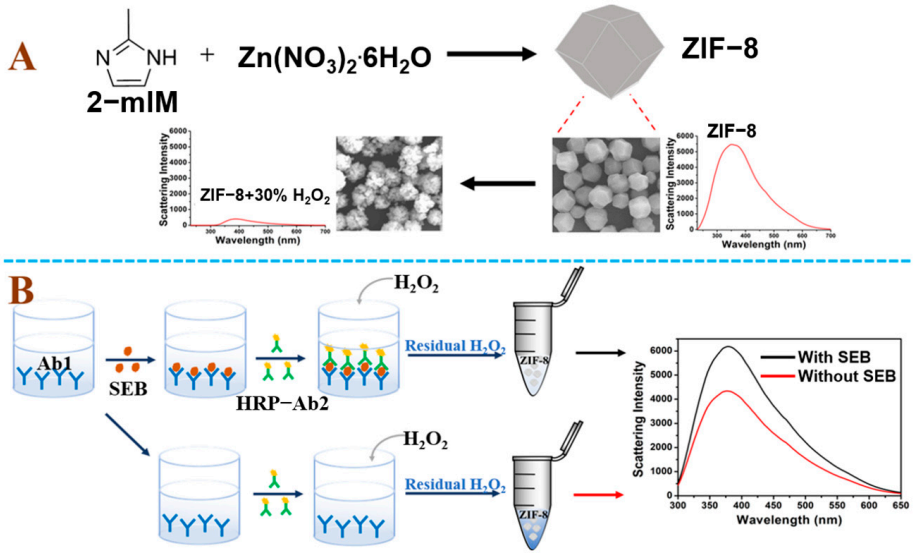

Figure 1. (**A**) Schematic illustration of the synthesis of ZIF-8 and the reaction between H_2O_2 and ZIF-8. (**B**) Schematic illustration of SEB detection.

3.2. Characterization of ZIF-8 and Its Reaction with H_2O_2

The as-prepared ZIF-8 was characterized using Fourier transform infrared (FTIR) and X-ray diffraction (XRD) measurements. In the absorption FTIR spectra of ZIF-8, peaks at 3138 cm^{-1} and 2933 cm^{-1} belong to the stretching vibration of C−H in methyl and imidazole rings, respectively (Figure 2A). The XRD studies (Figure 2B) showed that ZIF-8 had multiple diffraction peaks, mainly consisting of 2θ = 7.3°, 10.2°, 12.5°, 14.5°, 16.2°, 17.8°, 21.8°, etc. The above angles corresponded to planes (011), (002), (112), (022), (013), (222), and (114), respectively, with the sharpest peak at 2θ = 7.3 °, indicating that the synthesized ZIF-8 has a higher crystallinity. These results confirmed that the ZIF-8 with a higher crystallinity was synthesized successfully.

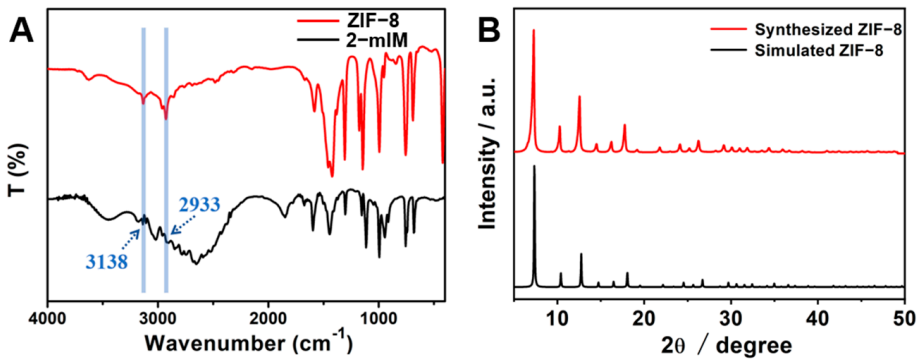

Figure 2. Characterization of ZIF-8. (**A**) Fourier transform infrared (FTIR); (**B**) X-ray diffraction (XRD).

Subsequently, we measured the LS spectra of ZIF-8 before and after the addition of H_2O_2 with different concentrations (Figure S1), and with the increase in the concentration of H_2O_2, the LS intensity of ZIF-8 showing an obvious downward trend was observed. Because H_2O_2 could destroy the structure of ZIF-8, so the LS intensity decreased significantly.

The morphology of ZIF-8 before and after the reaction with different concentrations of H_2O_2 was further characterized using scanning electron microscopy (SEM). As shown in Figure 2, ZIF-8 presented a regular dodecahedron structure (Figure 3A). After the

reaction with 0.1% H_2O_2, the regular morphology of ZIF-8 was destroyed (Figure 3B). With the increase in H_2O_2 concentration, the degree of destruction of ZIF-8 also increased (Figure 3C,D). These results directly confirmed that H_2O_2 can destroy the structure of ZIF-8.

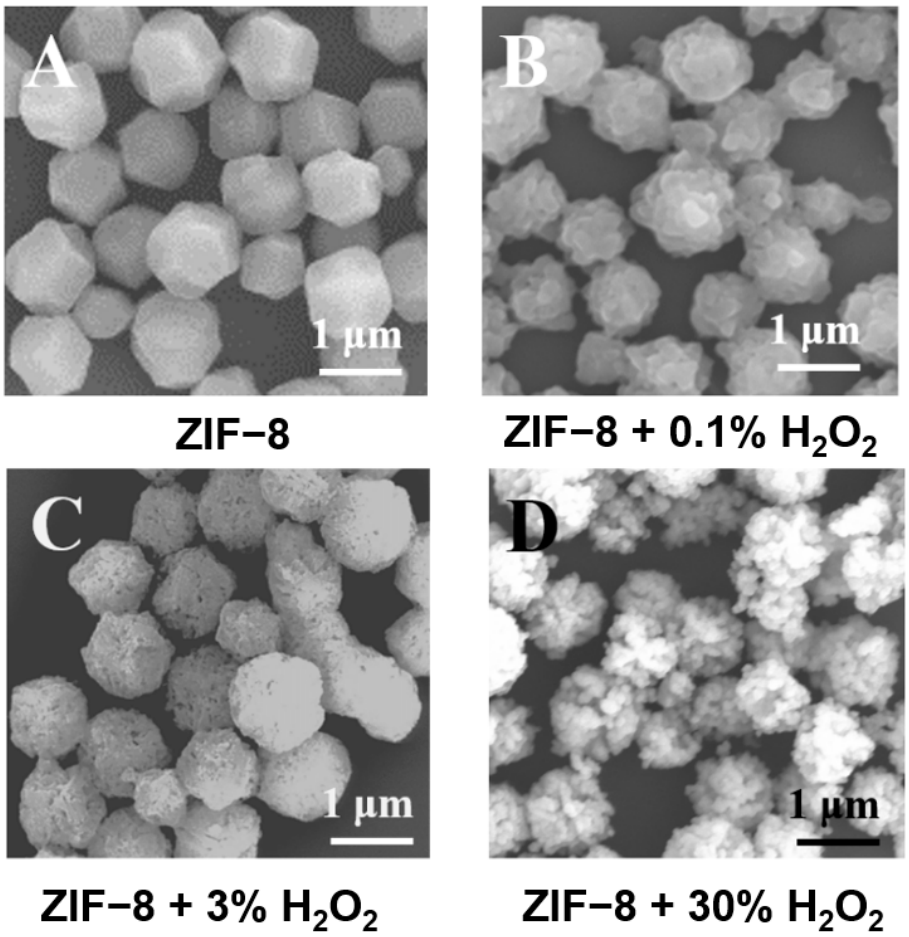

Figure 3. The SEM image of ZIF-8 before (**A**) and after the reaction with 0.1% H_2O_2 (**B**), 3% H_2O_2 (**C**), and 30% H_2O_2 (**D**). Experimental conditions: concentration of ZIF-8, 50 μg/mL; reaction time, 70 min.

We also investigated the dark field microscopic (DFM) images of ZIF-8 before and after the reaction with H_2O_2. As shown in Figure 4A, the DFM image of ZIF-8 showed an obvious doughnut-shaped image, and the LS intensity at the edge of the DFM image of ZIF-8 was very strong. However, after the reaction with 30% H_2O_2, the doughnut-shaped image changed into the solid scattering light spot, and the LS intensity decreased significantly (Figure 4B). Then, in situ DFM imaging was conducted for real-time monitoring of the reaction between ZIF-8 and H_2O_2. As shown in Figure 4C, with the addition of H_2O_2, the size and intensity of dark field scattering spots of ZIF-8 gradually decreased with the extension of incubation time. These results further proved that H_2O_2 could destroy ZIF-8, resulting in the reduction of the LS intensity of ZIF-8.

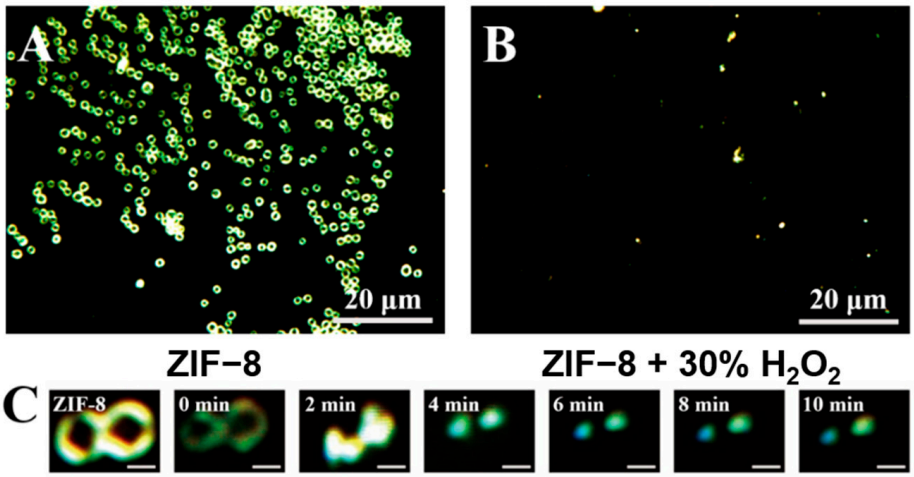

Figure 4. The dark field characterization of ZIF-8 reaction with H_2O_2. (**A**) The dark field characterization of ZIF-8. (**B**) The dark field characterization of ZIF-8 reaction with 30% H_2O_2. Experimental conditions: the concentration of ZIF-8 in A and B was 50 μg/mL; and the reaction time between ZIF-8 and 30% H_2O_2 was 70 min. The scale bar was 20 μm. (**C**) Real-time monitoring of the dark field light scattering image of the ZIF-8 and H_2O_2 reaction processes. Experimental conditions: the concentration of H_2O_2 was 3%. The scale bar was 1 μm.

3.3. LS Spectral Characteristics of ZIF-8 for SEB Detection

To investigate whether the proposed method could be applied for the detection of SEB, the LS spectral characteristics of ZIF-8 before and after the addition of SEB was measured. As shown in Figure 5A, in the presence of SEB, the LS intensity of ZIF-8 was significantly higher than that of the control group before adding SEB. The Ab1/SEB/Ab2-HRP sandwich immune complex structure was formed in the 96-well plate after the addition of SEB. Although HRP can react with H_2O_2 to produce OH·, only the remaining H_2O_2 can react with ZIF-8 because of the short life of OH· [35]. Compared with the system without SEB, the H_2O_2 content decreased and the oxidation capacity of ZIF-8 ligand 2-mIM decreased with the addition of SEB, so ZIF-8 maintained higher scattering intensity. Therefore, SEB could be detected by the significantly enhanced LS intensity at 378 nm (Figure 5B).

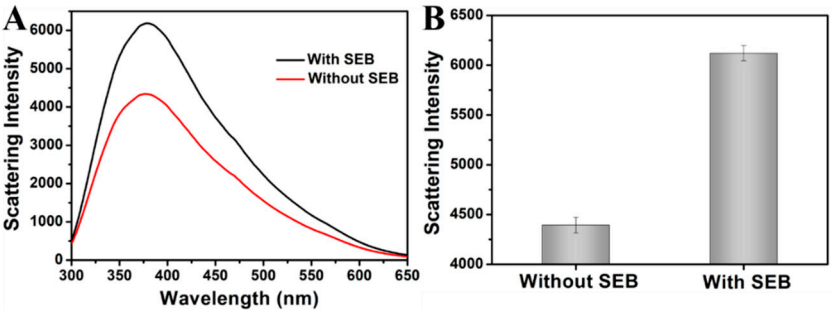

Figure 5. LS spectrum (**A**) and intensity at 378 nm (**B**) of ZIF-8 before and after the addition of SEB. Experimental conditions: the concentration of SEB in A and B was 1000 ng/mL; reaction time, 70 min; ZIF-8, 50 μg/mL; H_2O_2, 3%. The error bars represent the standard deviation of three replicates.

3.4. Optimization of the SEB Detection Conditions

In order to obtain excellent analytical performance, some important experimental conditions were optimized. We first optimized the reaction time of ZIF-8 with H_2O_2. As shown in Figure 6A, when the reaction time was 70 min, the light scattering signal difference (ΔI), which was calculated by subtracting the scattering intensity of ZIF-8 before

adding SEB from that after the addition of SEB, reached the maximum. Thus, 70 min was selected as the best reaction time. Subsequently, we optimized the concentration of H_2O_2. As shown in Figure 6B, when H_2O_2 concentration was 3%, ΔI was the largest, and 3% H_2O_2 was selected as the best reaction condition. Finally, we optimized the concentration of ZIF-8. The low concentration of ZIF-8 will result in low LS intensity and small signal changes. However, high concentrations of ZIF-8 can also affect the detection sensitivity. As shown in Figure 6C, when ZIF-8 concentration was 10–50 μg/mL, ΔI showed an upward trend. When ZIF-8 concentration was 50–90 μg/mL, ΔI showed a downward trend. Therefore, 50 μg/mL was finally selected as the optimal concentration of ZIF-8.

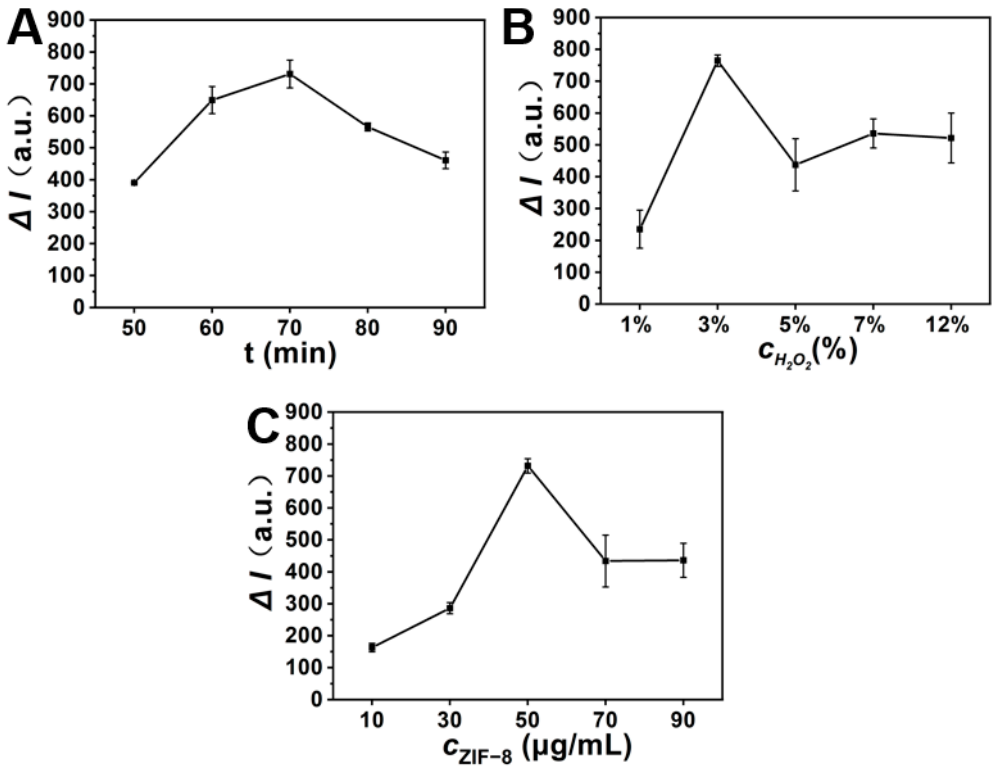

Figure 6. Optimization of the SEB detection conditions (**A**). The effect of the reaction time with ZIF-8 and H_2O_2 (**B**). The effect of the concentrations of H_2O_2 (**C**). The effect of the concentration of ZIF-8. Experimental conditions: the concentration of SEB in (**A**–**C**) was 250 ng/mL. The error bars represent the standard deviation of three replicates.

3.5. Analytical Performance of SEB Detection

Under optimal experimental conditions, the sensitivity of the method was investigated. As shown in Figure 7, the LS intensity variation and SEB concentration showed a good linear relationship within the range of 7–500 ng/mL. The linear regression equation was ΔI = 2.982 c_{SEB} + 33.575 (R^2 = 0.998), and the limit of detection (LOD, 3 σ/k) was 0.69 ng/mL. This method is more sensitive to the response of SEB, as shown in Table 1. The detection limit of this method is still comparable to some reported methods.

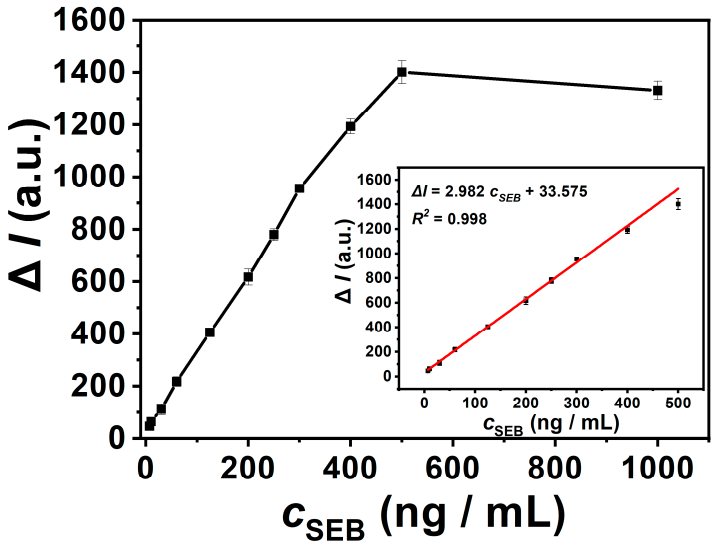

Figure 7. Linearity of SEB detection. The inset is the linear relationship between Δ*I* and SEB concentration (7 ng/mL to 500 ng/mL). Experimental conditions: the concentration of SEB was from 7 ng/mL to 1000 ng/mL; reaction time, 70 min; ZIF-8, 50 μg/mL; H_2O_2, 3%. The error bars represent the standard deviation of three replicates. The black line represents that Δ*I* increases with the increase of SEB concentration until reaching the plateau period. The black line represents the linear range.

Table 1. Current advances in selective detection of SEB with different test methods.

Test Methods	LOD	Ref.
Spectral method	0.5 ng/mL	[5]
SERS-lateral flow immunoassay	0.05 ng/mL	[36]
Enzyme-linked immunosorbent assay	0.38 ng/mL	[37]
Raman spectroscopy and chemometric methods	0.2 ng/L	[38]
Light scattering ELISA	0.69 ng/mL	This work

Then, we examined the selectivity of this platform for the detection of SEB. Under the same experimental conditions, we compared the response signals of this method to aflatoxin B1 (AFB1), hemoglobin (HGB), ochratoxin A (OTA), staphylococcal enterotoxin A (SEA), carcinoembryonic antigen (CEA), bovine serum albumin (BSA), and SEB. As shown in Figure 8A, the LS intensity difference produced by SEA, AFB1, OTA, BSA, HGB, and CEA was very low, and only the presence of SEB could lead to an obvious value of Δ*I*. These experimental results illustrated that this method had a good selectivity for the detection of SEB.

Since various potential substances in actual samples may affect the detection results, we investigated the influence of HCO_3^-, I^-, K^+, Na^+, Zn^{2+}, Ca^{2+}, Ba^{2+}, Fe^{2+}, Fe^{3+}, Al^{3+}, glucose, sucrose, Congo Red, and other substances on SEB detection. The concentrations of interferences (2500 ng/mL) were 10 times than that of SEB (250 ng/mL). The experimental results are shown in Figure 8B. The potential interfering substances had no significant influence on the detection of SEB.

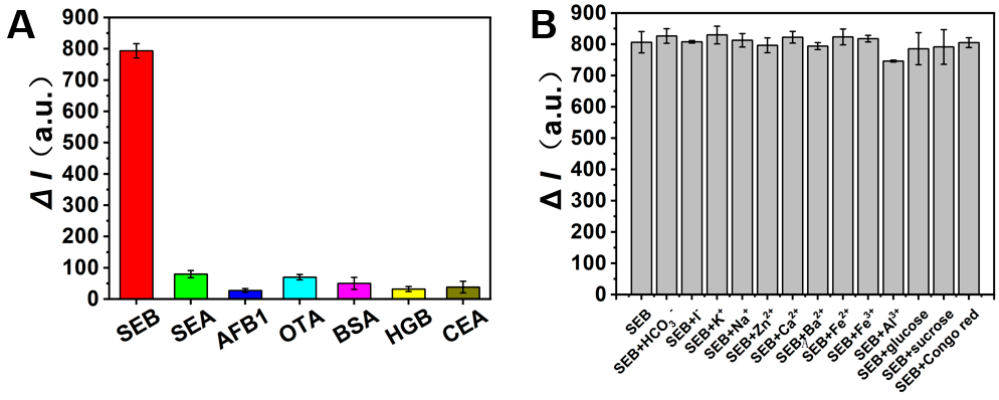

Figure 8. Selectivity of the proposed strategy (**A**). The concentration of SEB, SEA, AFB1, OTA, BSA, HGB, and CEA were 250 ng/mL; The effect of various interfering substances on the detection of SEB (**B**). The concentrations of SEB was 250 ng/mL and other substances were 2500 ng/Ml. Experimental conditions: reaction time, 70 min; ZIF-8, 50 μg/mL; H_2O_2, 3%. The error bars represent the standard deviation of three replicates.

In addition, we focus on exploring the influence of colored samples on colorimetric materials. As shown in the Figure S1, we washed the 96-well plate for 0 to 5 times, and then tested the SEB using both SEB ELISA test kits and light scattering ELISA. Under the linear range, the concentration of SEB used by the SEB ELISA test kits is 5 pg/mL, the concentration of Congo Red is 50 pg/mL, the concentration of SEB used by the light scattering ELISA is 250 ng/mL, and the concentration of Congo Red is 2500 ng/mL. After several plate washing operations, the detection results obtained using the SEB ELISA detection kits were all higher than the actual concentration (Figure S2A); The detection results obtained by the light scattering ELISA method after the fourth plate washing operation were consistent with the actual concentration (Figure S2B). Therefore, light scattering ELISA has greater advantages in the detection of colored samples.

3.6. SEB Detection in Complex Samples

We carried out the standard recovery experiment of SEB in orange juice, fresh milk, and skim milk powder to test whether this method could be applied in the real sample detection. Firstly, three different concentrations of SEB were added to the orange juice and detected by our method. The accuracy of this method for SEB detection was evaluated by Recovery. As shown in Table 2, the spiked recoveries of SEB in orange juice were 91.9–106.2%, and the relative standard deviations (RSD) were 2.10–8.21%, indicating that this method could be used for the detection of SEB in orange juice. Furthermore, the concentrations of SEB in fresh milk and skim milk powder were tested. Dissolve 200 mg skim milk powder in 1 mL sample diluent as its initial concentration. The recovery of SEB detection in fresh milk was 92.0–109.6% with RSD of 0.16–9.25%, and in skim milk powder, it was 90.2–107.0% with RSD of 1.45–6.85%. These results indicated that this method has good accuracy in the detection of SEB in different food substrates.

Table 2. Recovery tests of SEB detection in food matrices.

Sample	Added (ng/mL)	Found (ng/mL) Mean [a] ± SD [b]	Recovery (%, *n* = 3)	RSD (%, *n* = 3)
Orange juice	400	403.5 ± 8.46	98.9–103.2	8.21
	250	251.3 ± 12.3	96.9–106.2	4.91
	60	60.9 ± 5.0	91.9–106.5	2.10

Table 2. *Cont.*

Sample	Added (ng/mL)	Found (ng/mL) Mean [a] ± SD [b]	Recovery (%, *n* = 3)	RSD (%, *n* = 3)
Fresh milk	400	397.2 ± 36.73	92.0–109.6	9.25
	250	250.5 ± 16.61	93.4–106.7	6.63
	60	60.3 ± 0.97	98.6–101.4	0.16
Milk powder	400	369.0 ± 12.24	90.2–95.8	3.32
	250	257.0 ± 3.73	101.5–104.4	1.45
	60	59.5 ± 4.08	94.7–107.0	6.85

[a] The mean of three determinations. [b] SD The standard deviation.

3.7. Staphylococcal Enterotoxin A (SEA) Detection

Finally, in order to investigate the universality of this method, we applied it for the detection of staphylococcal enterotoxin A (SEA) by changing the corresponding recognition units. Quantitative detection of SEA can be achieved by the obviously changed LS intensity of ZIF-8 before and after adding SEA. As can be seen from Figure 9A, Δ*I* gradually increases with the increase in concentration of SEA. The experimental results showed that there was a linear relationship between the Δ*I* with the concentration of SEA at the range of 30 ng/mL–70 ng/mL. The linear equation was $\Delta I = 29.042\ c_{SEA} - 442.509$ ($R^2 = 0.991$), and the limit of detection (LOD, 3 σ/k) was 1.58 ng/mL.

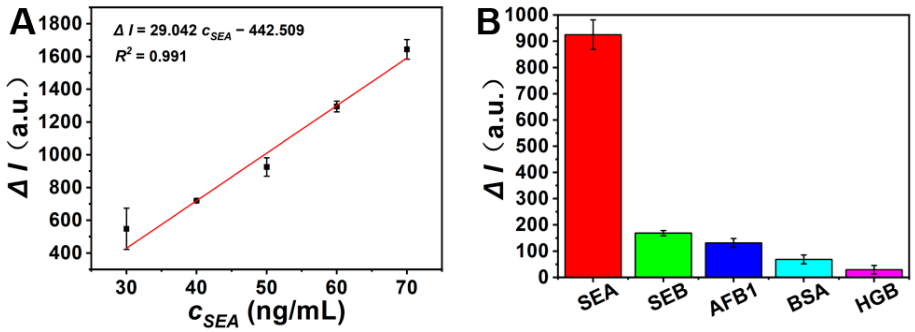

Figure 9. Linearity of SEA detection (**A**). The inset is the linear relationship between Δ*I* and SEA concentration (30 ng/mL to 70 ng/mL). Selectivity of the proposed strategy (**B**). Experimental conditions: the concentration of SEB was from 30 ng/mL to 70 ng/mL; the concentration of SEB, AFB1, BSA, and HGB were 50 ng/mL; reaction time, 70 min; ZIF-8, 50 μg/mL; H_2O_2, 3%. The error bars represent the standard deviation of three replicates.

Then, the selectivity of the method was tested by comparing the signal generated by SEA, staphylococcal enterotoxin B (SEB), aflatoxin B1 (AFB1), bovine serum albumin (BSA), and hemoglobin (HGB) at the same concentration. It was found that only SEA induced a high ΔI value (Figure 9B), indicating that the method could be used for the specific detection of SEA. These results confirmed that this method is universal.

4. Conclusions

ZIF-8 MOF was synthesized and employed as a new LS reporter of the ELISA for the detection of SEB based on the unique reaction of ZIF-8 MOF and H_2O_2. This developed LS ELISA method has several advantages. Firstly, the synthesis of ZIF-8 is easy. Secondly, the structure of the synthesized ZIF-8 was uniform, and its LS signal was strong and stable. Thirdly, compared with commercial SEB ELISA test kits, light scattering ELISA shows more reliable properties for the detection of colored samples, and the operation steps can be further simplified. Furthermore, this method does not need strong acid to stop the reaction, and the experimental operation is safer. Therefore, this method has been successfully applied for the direct detection of SEB in complex food samples. We

believe this method could be extended to the detection of other biotoxins by changing the corresponding antibodies.

Supplementary Materials: The following supporting information can be downloaded at: https://www.mdpi.com/article/10.3390/chemosensors11080453/s1, Figure S1: The reaction between ZIF-8 and H_2O_2. (A) The LS spectrum of ZIF-8 before and after the reaction with H_2O_2. (B) The LS intensity of ZIF-8 before and after the reaction with H_2O_2. Experimental conditions: the concentration of H_2O_2 in A and B was 0.1%, 3%, 30%; reaction time, 70 min; ZIF-8, 50 μg/mL. The error bars represent the standard deviation of three replicates. Figure S2: SEB ELISA test kits test results (A). The concentration of SEB is 5 pg/mL, the concentration of Congo Red is 50 pg/mL. and the light scattering ELISA test results (B). The concentration of SEB is 250 ng/mL, and the concentration of Congo Red is 2500 ng/mL. Among them, 0 to 5 represent the number of times the board is washed; The error bars represent the standard deviation of three replicates.

Author Contributions: Investigation, Data curation, Validation, Formal analysis, Writing—original draft, K.M.; Investigation, Methodology, Writing—original draft, Writing—review and editing, L.T.; Methodology, Writing—original draft, Writing—review and editing, Y.L. (Yujie Luo); Validation, Data curation and Formal analysis, Q.L.; Validation, Data curation and Formal analysis, X.C.; Writing—review and editing, L.Z., Y.L. (Yuanfang Li), C.H. and S.Z.; Methodology, Funding Acquisition, Supervision, S.Z. All authors have read and agreed to the published version of the manuscript.

Funding: This work was supported by National Natural Science Foundation of China (No. 21974109), the Natural Science Foundation of Chongqing (No. CSTB2022NSCQ-MSX1662), and Fundamental Research Funds for the Central Universities (XDJK2019TY003).

Institutional Review Board Statement: Not applicable.

Informed Consent Statement: Not applicable.

Data Availability Statement: Data are contained within the article and Supplementary Materials.

Acknowledgments: The authors would like to thank the Key Laboratory of Luminescence Analysis and Molecular Sensing (Southwest University) for supporting this research and providing the appropriate research environment.

Conflicts of Interest: The authors declare no conflict of interest.

References

1. Mousavi, N.S.; Nasirizadeh, N.; Amani, J.; Halabian, R.; Fooladi, I.A.A. An electrochemical aptasensor for staphylococcal enterotoxin B detection based on reduced graphene oxide and gold nano-urchins. *Biosens. Bioelectron.* **2019**, *127*, 221–228. [CrossRef] [PubMed]
2. Sospedra, I.; Marín, R.; Mañes, J.; Soriano, J.M. Rapid whole protein quantification of staphylococcal enterotoxin B by liquid chromatography. *Food Chem.* **2012**, *133*, 163–166. [CrossRef]
3. Muratovic, A.Z.; Hagstrom, T.; Rosen, J.; Granelli, K.; Hellenas, K.E. Quantitative Analysis of Staphylococcal Enterotoxins A and B in Food Matrices Using Ultra High-Performance Liquid Chromatography Tandem Mass Spectrometry (UPLC-MS/MS). *Toxins* **2015**, *7*, 3637–3656. [CrossRef]
4. Andjelkovic, M.; Tsilia, V.; Rajkovic, A.; De Cremer, K.; Van Loco, J. Application of LC-MS/MS MRM to Determine Staphylococcal Enterotoxins (SEB and SEA) in Milk. *Toxins* **2016**, *8*, 118. [CrossRef] [PubMed]
5. Kumari, S.; Tiwari, M.; Das, P. Multi format compatible visual and fluorometric detection of SEB toxin in nanogram range by carbon dot-DNA and acriflavine nano-assembly. *Sens. Actuators B* **2019**, *279*, 393–399. [CrossRef]
6. Xiong, X.; Shi, X.; Liu, Y.; Lu, L.; You, J. An aptamer-based electrochemical biosensor for simple and sensitive detection of staphylococcal enterotoxin B in milk. *Anal. Methods* **2018**, *10*, 365–370. [CrossRef]
7. Wang, W.; Wang, W.; Liu, L.; Xu, L.; Kuang, H.; Zhu, J.; Xu, C. Nanoshell-Enhanced Raman Spectroscopy on a Microplate for Staphylococcal Enterotoxin B Sensing. *ACS Appl. Mater. Interfaces* **2016**, *8*, 15591–15597. [CrossRef] [PubMed]
8. Xue, P.; Li, Y.; Zhang, Z.; Fu, A.; Liu, F.; Zhang, X.; Sun, Y.; Chen, L.; Jin, B.; Yang, K. Novel chemiluminescent assay for staphylococcal enterotoxin B. *Microchim. Acta* **2011**, *174*, 167–174. [CrossRef]
9. Lu, B.; Bai, J.; Zhang, J.; Shen, H.; Wang, M.; Lian, Y.; Gao, Z.; Peng, Y. Iridescent polymeric film with tunable color responses to ultra-trace Staphylococcus aureus enterotoxin B. *Sensor. Actuat. B—Chem.* **2023**, *380*, 133318. [CrossRef]
10. Margalit, Y.; Lu, Y.K.; Top, F.C.; Ketterle, W. Pauli blocking of light scattering in degenerate fermions. *Science* **2021**, *374*, 976–979. [CrossRef]
11. Celiksoy, S.; Ye, W.; Wandner, K.; Kaefer, K.; Sönnichsen, C. Intensity-Based Single Particle Plasmon Sensing. *Nano Lett.* **2021**, *21*, 2053–2058. [CrossRef] [PubMed]

12. Gao, H.; Wu, P.; Song, P.; Kang, B.; Xu, J.J.; Chen, H.Y. The video-rate imaging of sub-10 nm plasmonic nanoparticles in a cellular medium free of background scattering. *Chem. Sci.* **2021**, *12*, 3017–3024. [CrossRef]
13. Wang, J.C.; Wang, Y.S.; Xue, J.H.; Zhou, B.; Qian, Q.M.; Wang, Y.S.; Yin, J.C.; Zhao, H.; Liu, H.; Liu, S.D. An ultrasensitive label-free assay of 8-hydroxy-2′-deoxyguanosine based on the conformational switching of aptamer. *Biosens. Bioelectron.* **2014**, *58*, 22–26. [CrossRef] [PubMed]
14. Wang, J.; Li, T.; Shen, R.; Li, G.; Ling, L. Polymerase Chain Reaction-Dynamic Light Scattering Sensor for DNA and Protein by Using Both Replication and Cleavage Properties of Taq Polymerase. *Anal. Chem.* **2019**, *91*, 3429–3435. [CrossRef] [PubMed]
15. Zou, L.; Ling, L. Ultrasensitive Detection of HIV DNA with Polymerase Chain Reaction-Dynamic Light Scattering. *Anal. Chem.* **2018**, *90*, 13373–13377. [CrossRef] [PubMed]
16. El-Kurdi, R.; Patra, D. Gold and silver nanoparticles in resonance Rayleigh scattering techniques for chemical sensing and biosensing: A review. *Mikrochim. Acta* **2019**, *186*, 667. [CrossRef]
17. Hu, P.; Huang, C.Z.; Li, Y.F.; Liang, J.; Liu, Y.L.; Fei, L.R.; Xie, J.P. Magnetic Particle-Based Sandwich Sensor with DNA-Modified Carbon Nanotubes as Recognition Elements for Detection of DNA Hybridization. *Anal. Chem.* **2008**, *80*, 1819–1823. [CrossRef]
18. Qi, W.J.; Wu, D.; Ling, J.; Huang, C.Z. Visual and light scattering spectrometric detections of melamine with polythymine-stabilized gold nanoparticles through specific triple hydrogen-bonding recognition. *Chem. Commun.* **2010**, *46*, 4893–4895. [CrossRef]
19. Feng, D.Q.; Liu, G.; Wang, W. A novel biosensor for copper(ii) ions based on turn-on resonance light scattering of ssDNA templated silver nanoclusters. *J. Mater. Chem. B* **2015**, *3*, 2083–2088. [CrossRef]
20. Kohli, R.K.; Davies, J.F. Measuring the Chemical Evolution of Levitated Particles: A Study on the Evaporation of Multicomponent Organic Aerosol. *Anal. Chem.* **2021**, *93*, 12472–12479. [CrossRef]
21. Latimer, P.; Barber, P. Scattering by ellipsoids of revolution a comparison of theoretical methods. *J. Colloid Interface Sci.* **1978**, *63*, 310–316. [CrossRef]
22. Al-Chalabi, S.A.M.; Jones, A.R. Light scattering by irregular particles in the Rayleigh-Gans-Debye approximation. *J. Phys. D Appl. Phys.* **1995**, *28*, 1304. [CrossRef]
23. Ling, J.; Li, Y.F.; Huang, C.Z. Visual Sandwich Immunoassay System on the Basis of Plasmon Resonance Scattering Signals of Silver Nanoparticles. *Anal. Chem.* **2009**, *81*, 1707–1714. [CrossRef]
24. Ling, J.; Huang, C.Z.; Li, Y.F.; Zhang, L.; Chen, L.Q.; Zhen, S.J. Light-scattering signals from nanoparticles in biochemical assay, pharmaceutical analysis and biological imaging. *TrAC* **2009**, *28*, 447–453. [CrossRef]
25. Pasternack, R.F.; Bustamante, C.; Collings, P.J.; Giannetto, A.; Gibbs, E.J. Porphyrin Assemblies on DNA as Studied by a Resonance Light-Scattering Technique. *J. Am. Chem. Soc.* **1993**, *115*, 5393–5399. [CrossRef]
26. Zhao, X.; Wang, Y.; Li, D.S.; Bu, X.; Feng, P. Metal-Organic Frameworks for Separation. *Adv. Mater.* **2018**, *30*, e1705189. [CrossRef] [PubMed]
27. Terzopoulou, A.; Nicholas, J.D.; Chen, X.Z.; Nelson, B.J.; Pane, S.; Puigmarti-Luis, J. Metal-Organic Frameworks in Motion. *Chem. Rev.* **2020**, *120*, 11175–11193. [CrossRef]
28. Troyano, J.; Carne-Sanchez, A.; Avci, C.; Imaz, I.; Maspoch, D. Colloidal metal-organic framework particles: The pioneering case of ZIF-8. *Chem. Soc. Rev.* **2019**, *48*, 5534–5546. [CrossRef]
29. Saliba, D.; Ammar, M.; Rammal, M.; Al-Ghoul, M.; Hmadeh, M. Crystal Growth of ZIF-8, ZIF-67, and Their Mixed-Metal Derivatives. *J. Am. Chem. Soc.* **2018**, *140*, 1812–1823. [CrossRef]
30. He, L.Z.; Huang, G.N.; Liu, H.X.; Sang, C.C.; Liu, X.X.; Chen, T.F. Highly bioactive zeolitic imidazolate framework-8–capped nanotherapeutics for efficient reversalofreperfusion-induced injury in ischemic stroke. *Sci. Adv.* **2020**, *6*, 9751. [CrossRef]
31. Hu, X.; Liu, X.; Zhang, X.; Chai, H.; Huang, Y. One-pot synthesis of the CuNCs/ZIF-8 nanocomposites for sensitively detecting H(2)O(2) and screening of oxidase activity. *Biosens. Bioelectron.* **2018**, *105*, 65–70. [CrossRef]
32. Carraro, F.; Williams, J.D.; Linares-Moreau, M.; Parise, C.; Liang, W.; Amenitsch, H.; Doonan, C.; Kappe, C.O.; Falcaro, P. Continuous-Flow Synthesis of ZIF-8 Biocomposites with Tunable Particle Size. *Angew. Chem. Int. Ed. Engl.* **2020**, *59*, 8123–8127. [CrossRef]
33. Lee, Y.R.; Jang, M.S.; Cho, H.Y.; Kwon, H.J.; Kim, S.; Ahn, W.S. ZIF-8: A comparison of synthesis methods. *Chem. Eng. J.* **2015**, *271*, 276–280.
34. Hu, P.; Zhuang, J.; Chou, L.Y.; Lee, H.K.; Ling, X.Y.; Chuang, Y.C.; Tsung, C.K. Surfactant-directed atomic to mesoscale alignment: Metal nanocrystals encased individually in single-crystalline porous nanostructures. *J. Am. Chem. Soc.* **2014**, *136*, 10561–10564. [CrossRef]
35. Attri, P.; Kim, Y.H.; Park, D.H.; Park, J.H.; Hong, Y.J.; Uhm, H.S.; Kim, K.N.; Fridman, A.; Choi, E.H. Generation mechanism of hydroxyl radical species and its lifetime prediction during the plasma-initiated ultraviolet (UV) photolysis. *Sci. Rep.* **2015**, *5*, 9332. [CrossRef] [PubMed]
36. Jia, X.; Wang, K.; Li, X.; Liu, Z.; Liu, Y.; Xiao, R.; Wang, S. Highly sensitive detection of three protein toxins via SERS-lateral flow immunoassay based on SiO(2)@Au nanoparticles. *Nanomedicine* **2022**, *41*, 102522. [CrossRef]

37. Jang, J.H.; Kim, S.; Kim, S.G.; Lee, J.; Lee, D.G.; Jang, J.; Jeong, Y.S.; Song, D.H.; Min, J.K.; Park, J.G.; et al. A Sensitive Immunodetection Assay Using Antibodies Specific to Staphylococcal Enterotoxin B Produced by Baculovirus Expression. *Biosensors* **2022**, *12*, 787. [CrossRef] [PubMed]
38. Du, Y.; Huang, H.; Peng, Y.; Wang, J.; Gao, Z. Rapid determination of Staphylococcus aureus enterotoxin B in milk using Raman spectroscopy and chemometric methods. *J. Raman Spectrosc.* **2022**, *53*, 709–714. [CrossRef]